THE JOURNAL OF BIOLOGICAL CHEMISTRY VOL. 288, NO. 39, pp. 28398–28408, September 27, 2013

Galectin-3 Guides Intracellular Trafficking of Some Human Serotransferrin Glycoforms*

Received for publication, May 24, 2013, and in revised form, August 6, 2013 Published, JBC Papers in Press, August 7, 2013, DOI 10.1074/jbc.M113.487793

Michael C. Carlsson[‡1], **Per Bengtson**[§], **Helena Cucak**[‡], **and Hakon Leffler**[‡2]

From the [‡]*Section MIG (Microbiology, Immunology, Glycobiology), Department of Laboratory Medicine and the* [§]*Division of Clinical Chemistry and Pharmacology, 221 00 Lund University, Lund, Sweden*

Background: Transferrin has two *N*-glycans but their biological function remains unknown.
Results: About 5% of human serotransferrin glycoforms bind galectin-3 and are targeted to a different endocytic pathway.
Conclusion: Transferrin glycosylation may mediate a previously unrecognized level of physiological regulation.
Significance: This is the first evidence that different molecular forms of transferrin, besides iron loading, may have different cellular function.

Transferrin internalization via clathrin-mediated endocytosis and subsequent recycling after iron delivery has been extensively studied. Here we demonstrate a previously unrecognized parameter regulating this recycling, the binding of galectin-3 to particular glycoforms of transferrin. Two fractions of transferrin, separated by affinity chromatography based on their binding or not to galectin-3, are targeted to kinetically different endocytic pathways in HFL-1 cells expressing galectin-3 but not in SKBR3 cells lacking galectin-3; the SKBR3 cells, however, can acquire the ability to target these transferrin glycoforms differently after preloading with exogenously added galectin-3. In all, this study provides the first evidence of a functional role for transferrin glycans, in intracellular trafficking after uptake. Moreover, the galectin-3-bound glycoform increased in cancer, suggesting a pathophysiological regulation. These are novel aspects of transferrin cell biology, which has previously considered only a degree of iron loading, but not other forms of heterogeneity.

Human serum transferrin is a glycoprotein synthesized mainly by hepatocytes and is involved in iron transport between sites of absorption and delivery. Transferrin endocytosis is considered to be a classic example of clathrin-mediated internalization, entry into early endosomes, and subsequent recycling back to the cell membrane. During this cycle, iron is released into the endosomal compartment (1). Transferrin appears to be recycled by two main kinetically distinct pathways: one rapid recycling via early endosomes, and one slower with additional passage through late and recycling endosomes before returning to the cell membrane (2–4). The regulation of these pathways by proteins acting at the cytosolic side of the plasma membrane and vesicles has been studied extensively. However, except for iron loading (5, 6) and interaction with cellular transferrin receptors (7), there has been no study on the possible regulatory effect of properties of transferrin itself, such as its different glycoforms.

Transferrin has two potential *N*-glycosylation sites, usually with two bi- and/or triantennary *N*-glycans. Transferrin glycoforms have been analyzed extensively as surrogate markers for rare genetic disorders of glycosylation, and also for alcohol-induced liver injury (8). However, the biological significance of the two glycans in respect to transferrin function is not fully understood. We recently found that a fraction (~5%) of normal transferrin is bound by galectin-3 (9), a member of a protein family defined by affinity for β-galactoside containing glycans, such as found in transferrin. Altered glycosylations are a hallmark of oncogenic transformation (10), and have been shown to alter galectin binding of glycoproteins (11–13). Galectin-3, like other galectins, has diverse roles in cancer, inflammation, and development (14), and one cellular mechanism for this is that it regulates the intracellular traffic of certain cellular glycoproteins by binding their glycans (11, 13, 15, 16). Therefore, we asked whether it could also direct the trafficking after endocytosis of an exogenous glycoprotein such as transferrin.

EXPERIMENTAL PROCEDURES

Expression and Purification of Galectins—Galectin-3 and galectin-3C were produced in *Escherichia coli* BL21 Star (Invitrogen) and purified by affinity chromatography on lactosyl-Sepharose as described earlier (17). The galectin-3 R186S mutant was previously constructed as described in Ref. 18.

Galectin Affinity Column—Galectin-3 was coupled to a 1- or 5-ml NHS-activated Hi-Trap affinity column (GE Healthcare) as described by the manufacturer, using 10 (1 ml column) or 40 mg (5 ml column) of galectin-3 in 2 or 10 ml of coupling buffer (0.2 M $NaHCO_3$, 0.5 M NaCl, pH 8.3). The total amount of galectin coupled to the column was obtained by subtracting the measured amount in the wash and circulating fractions from the initial amount added. 0.1 ml of serum in 1.9 ml of PBS or human transferrin (Sigma), dissolved in PBS to a final concentration of 3–4 mg/ml (total volume 5 ml), was kept on ice in a test tube and circulated on the column for 30 min at 1 (1 ml column) or 4 ml/min (5 ml column). The column was sealed for 30 min to enhance binding. The column was washed with 5

* The work was supported by grants from the Swedish Research Council (Vetenskapsrådet) and Region Skåne.
[1] To whom correspondence may be addressed: Dept. of Laboratory Medicine, Section MIG (Microbiology, Immunology, Glycobiology), Sölvegatan 23, S-223 62 Lund, Sweden. Tel.: 46-46-173273; Fax: 46-46-137468; E-mail: michael.carlsson@med.lu.se.
[2] To whom correspondence may be addressed. E-mail: hakon.leffler@med.lu.se.

column volumes of PBS and 1-ml fractions of the unbound fraction (flow-through) were saved. Galectin-3-binding proteins were eluted with 150 mM lactose in PBS and collected in 24 0.2-ml (1 ml column) or 1-ml (5 ml column) fractions. Protein concentrations of the collected fractions were determined with the Bio-Rad protein assay (Bio-Rad) and plotted in Prism software (GraphPad software) as a chromatogram.

Patient Samples—De-identified human serum samples were provided by Professor Mårten Fernö and Håkan Olsson, Department of Oncology, Lund University Hospital, Lund, Sweden, under ethical permit and approval from the Ethical Review Board at Lund University (Now Regional Ethical Review Board Lund). Written informed consent was obtained from all participants. All information and data were handled confidentially, and evaluation of information linked to patients was carried out in accordance with the Swedish Personal Data Act (Personuppgiftslagen in Swedish). Serum samples from 13 female metastatic breast cancer patients and 12 age-matched healthy female volunteers, listed in Table 1, were collected and stored as described previously (9, 19).

Transferrin Measurements—The amount of total serum transferrin and galectin-3-bound transferrin in pooled fractions from 13 female metastatic breast cancer patients and 12 age-matched healthy female volunteers was determined using a Transferrin Human ELISA Kit (Abcam) according to manufacturer's instructions.

Statistical Analysis—All pairwise comparisons between the cancer and control sera were done by a two-tailed unpaired *t* test using the GraphPad Prism software.

PHA-L[3] *Affinity Chromatography*— 400 μl of agarose-bound *Phaseolus vulgaris* leukoagglutinin (PHA-L) (1 mg/ml), were packed into a 1-ml syringe and equilibrated with PBS. 1 mg of human transferrin in a volume of 500 μl was added to the column and flow-through was collected in 200-μl fractions with continuous adding of PBS up to 15 ml. Possible retained protein was eluted using 0.1 M acetate buffer, pH 3. Protein concentrations of collected fractions were determined with the Bio-Rad protein assay (Bio-Rad) and plotted in Prism software (GraphPad software) as a chromatogram. Flow-through fractions were pooled based on retardation time and galectin-3 binding was determined by fluorescent anisotropy inhibition assay, described below.

LC-MS, Materials—POROS™-aldehyde self-pack medium was purchased from Applied Biosystems. Rabbit anti-human transferrin used in the immunoaffinity column was purchased from Dako. The C.128 precolumn (20 × 1 mm) and fittings used for immunoaffinity was purchased from Upchurch. Apotransferrin was purchased from Sigma. The C4 cartridge Widepore C4 (butyl); 4 × 2.0 mm (inner diameter) were bought from Phenomenex. All other chemicals and solvents were of the highest analytical grade available from commercial sources and were used without further purification.

Immunoaffinity Column Preparation—The method and preparation has been described before (20). In short, rabbit anti-human transferrin in phosphate-buffered saline (PBS; 0.01 mol/liter of phosphate, 0.150 M NaCl, pH 7.4) was mixed with 1.5 M Na_2SO_4, 100 mM phosphate, pH 7.4, followed by sodium cyanoborohydride. POROS-aldehyde self-pack medium was added and mixed. After incubation at RT the immobilized ligand was washed with PBS and capped with 0.2 M Tris, pH 7.2. After washing with PBS the resin was packed in C.128 columns.

LC-MS Analysis—The analysis was performed using an API 4000 triple quadrupole mass spectrometer (AB Sciex) equipped with the TurboIon Spray ionization probe source (operated at 5500 V). Peripherals included a CTC Autosampler, and a Shimadzu System Controller (SCL-10Avp), which controlled four Shimadzu Liquid Chromatography LC-10ADvp pumps. A 10-μl aliquot of sample was applied to the immunoaffinity column in PBS with 150 mM NaCl, pH 7.4, at a flow rate of 200 μl/min. Transferrin isoforms were subsequently eluted from the immunoaffinity column with 100 mM glycine, 2% acetic acid buffer (pH 2.5; flow rate, 200 ml/min) and concentrated on a C4 cartridge. The C4 column was then washed with 2 mM ammonium hydroxide, 28 mM formic acid in water:acetonitrile (98:2 by volume), pH 2.9, at a flow rate of 200 ml/min. Transferrin isoforms were eluted from the C4 column and introduced into the TurboIonSpray source using 28 mM formic acid in water: acetonitrile (2:98 by volume) at a flow rate of 200 ml/min. The mass spectrometer was operated in Q1 scan mode (m/z 2000 to 3000) with a transferrin retention time of 5 min and total instrument acquisition time of 6.5 min/sample. Data were acquired and processed using Analyst software (version 1.5.2; AB Sciex). The Bayesian protein reconstruct algorithm was used to deconvolute the charge distribution raw data to reconstructed mass data.

Iron Measurement—2 mg/ml (25 μM) of unseparated, galectin-3-unbound and -bound transferrin iron content was determined spectrophotometrically with the Ferene-S method as described (21) with a few exceptions. Absorbance was detected at 595 nm. Iron concentrations were determined by reference to a calibration curve generated from Fe^{3+} solutions in the range 0–50 μM. Ferene (3-(2-Pyridyl)-5,6-di(2-furyl)-1,2,4-triazine-5′,5″-disulfonic acid disodium salt) was purchased from (Sigma).

Neuraminidase Treatment—2 mg of human transferrin (Sigma) was treated with neuraminidase from *Vibrio cholerae* (Roche) (25 μmol/μmol of transferrin) for 1 h at 37 °C. Treated or untreated samples were then separated by affinity chromatography as described above.

NHS-fluorescein and NHS-sulforhodamine Labeling of Proteins—A 15-fold access of labeling dye, NHS-fluorescein or NHS-sulforhodamine (Thermo Scientific) dissolved in *N*,*N*-dimethylformamide was added to a 2 mg/ml of protein solution in 100 mM carbonate/bicarbonate buffer. The solution was mixed well and incubated for 1 h in room temperature. Labeled protein was separated from the unreacted dye by a buffer change to PBS on a PD10 column (Amersham Biosciences). Degree of labeling was calculated according to the manufacturer's instructions.

Cell Cultures—SKBR3 cells were grown in RPMI 1640 + L-glutamine supplemented with 1× sodium pyruvate and 1× non-essential amino acids. HFL-1 and MCF-7 cells were grown in DMEM (Invitrogen) culture medium. All culture media were

[3] The abbreviation used is: PHA-L, *Phaseolus vulgaris* leukoagglutinin.

supplemented with 10% fetal calf serum and 1% penicillin-streptomycin (Invitrogen), Complete medium. Humidified 37 °C incubators with 5% CO_2 were used for all cell incubations.

U18666A Treatment—For inhibition of recycling, HFL-1 and SKBR3 cells were pretreated with media containing 1 μg/ml of the class-2 amphiphile 3-β-[2-(diethylamino)ethoxy]-androst-5-en-17-one (U18666A) for 24 h.

Image Acquisition—Phase-contrast or epifluorescent images were captured using a Nikon eclipse TE2000-U fluorescence microscope with a CFI Plan Apochromat ×100 oil objective: numeric aperture 1.40, working distance 0.13 mm, and equipped with a digital still camera DS-Qi1MC. Fluorescent images (RGB, 8 bit, 1280 × 1024) were deconvolved from a three-dimensional stack (*x*,*y*,*z* dimensions: 129.82 × 103.85 × 21.6 μm) with NIS-element AR software. Percent colocalization was quantitated by two different approaches. 5 images of each individual experiment were examined using NIS-element AR software colocalization application and average values of overlap coefficients according to Manders were calculated after background correction with the same threshold in each image. In addition a minimum of 20 10-μm squares were randomly placed in the cytosol of a cell. The total number of X-positive endosomes (EEA1, Rab11, and LAMP-1) and the number of structures labeled by both X and transferrin within those squares was counted. The endosomes labeled by both markers were expressed as percentage of X-positive compartments. For each experiment at least three cells were counted.

Protein Endocytosis in HFL-1 and SKBR3 Cells—HFL-1 and SKBR3 cells were grown to 50–80% confluence in 24-well plates containing coverslips. Prior to addition of proteins cells were incubated for 30 min in serum-free medium. SKBR3 cells were in some experiments pretreated with galectin-3, galectin-3 R186S, or galectin-3C for 1 h up to 48 h. Following serum-free treatment or galectin pretreatment, cells were incubated with 1 μM variously labeled proteins (NHS-fluorescein and NHS-sulforhodamine-conjugated galectin-3 binding transferrin, NHS-fluorescein and NHS-sulforhodamine-conjugated galectin-3 non-binding transferrin, NHS-fluorescein and NHS-sulforhodamine-conjugated galectin-3, NHS-fluorescein-conjugated galectin-3 R186S and NHS-fluorescein-conjugated galectin-3C) in serum-free medium at 37 °C. Medium containing labeled protein was replaced with serum-free medium after 5 min in HFL-1 cells to stop constant uptake, whereas it remained in SKBR3 until endocytosis was stopped. Endocytosis was stopped by removing the medium followed by addition of ice-cold PBS and fixation in 2% paraformaldehyde. Coverslips were mounted using ProLong Antifade Reagent with DAPI or Moviol and 0.01 mg/ml of Hoechst before being analyzed with a Nikon eclipse TE2000-E fluorescence microscope.

Immunocytochemistry—Fixed cells were permeabilized with 500 μl of 1% Triton X-100 (Merck) in PBS for 10 min at room temperature. The cells were washed twice in ice-cold PBS before nonspecific binding was prevented by the addition of 500 μl of blocking buffer (0.1% Tween + 1% FBS in PBS) for 10 min at room temperature. Cells were incubated with 100 μl of primary antibodies: rat anti-mouse galectin-3 (1/100), mouse anti-human transferrin receptor CD71, mouse anti-human early endosomes specific protein EEA1 (1/250) (BD Bioscience), mouse anti-human lysosome-specific protein LAMP-1 (1:250) (Santa Cruz), and mouse anti-human Rab11 (1/100) for 1 h at room temperature. After three washes with PBS for 10 min, cells were incubated with 100 μl of secondary antibodies all diluted 1:320 in blocking buffer Alexa 488- and 594-conjugated anti-rat IgG (Sigma) and goat Alexa 488- and 594-conjugated anti-mouse IgG (Molecular Probes). Control staining with only the secondary antibody was performed to rule out eventual unspecific binding.

Western Blot—1×10^6 of HFL-1 or SKBR3 cells was dissolved in lysis buffer (0.9% NaCl, 2.4% Tris, 0.08% EDTA, 0.01% (v/v) Nonidet P-40) with addition of 2 μg/ml of protease inhibitors: leupeptin, aprotinin, and pepstain. After cell lysis, supernatants containing equal protein amounts were separated by denaturating SDS-PAGE on 4–20% polyacrylamide gel following the manufacturer's instructions (Pierce). Subsequently, the proteins were transferred to a PVDF methanol-activated membrane at 100 V for 1 h. To avoid unspecific binding, the membrane was incubated with blocking buffer (5% dry milk in PBS-T (1/15 M PBS, pH 7.2, + 1% Tween)) for 24 h. The membrane was then incubated in 1:1000 diluted rat anti-mouse galectin-3 or goat anti-human transferrin antibody in PBS-T for 1 h at room temperature. After washing (3 × 10 min), anti-rat or anti-goat horseradish peroxidase (HRP)-conjugated antibody in PBS-T was added at a 1:4000 dilution for 1 h at room temperature. Proteins were detected using an ECL Plus Western blotting detection system (GE Healthcare) for 5 min, and protein bands were scanned using a GelDoc imager (Bio-Rad). Band intensities from 5 parallel experiments were analyzed with ImageJ software.

Fluorescent Anisotropy Inhibition Assay—K_d of galectin-3-binding and non-binding transferrin and inhibitory potency of PHA-L flow-through fractions was determined using a fluorescent anisotropy inhibition assay using the different glycoforms of transferrin to inhibit the interaction of galectin-3 with a high affinity A-tetrasaccharide probe, as described in detail in Ref. 22.

Fluorescent Intensities in Cell Medium—To analyze endocytosis kinetics of galectin-3 and transferrin, fluorescence intensities in medium removed from SKBR3 cells at different time points was analyzed using POLARstar (excitation 485 nm/emission 520 nm (green) or excitation 570 nm/emission 610 nm (red)) with FLUOstar Galaxy version 4.11-0 software (BMG Lab-Technologies).

Flow Cytometry—MCF-7 cells were grown to a density of around 1×10^6 cells/ml and harvested using an enzyme-free cell dissociation solution (Chemicon International). Cells were incubated with 1 μM NHS-sulforhodamine-conjugated galectin-3-binding transferrin and allophycocyanin (APC) conjugated anti-galectin-3 (Biolegend) for 30 min. Cells were then kept untreated or treated with 150 mM lactose or 5 μM galectin-3 non-binding transferrin for 1 h followed by flow cytometry analysis using a FACS Fortessa (BD Biosciences). Data were analyzed using FACS Diva software (BD Biosciences). The cells were kept on ice throughout the experiment to prevent uptake.

RESULTS

Galectin-3 Binds a Small Fraction of Transferrin Enriched in Triantennary N-Glycans—Affinity chromatography of human transferrin on immobilized galectin-3 gave a bound fraction of about 5% that could be eluted as a sharp peak using lactose (Fig. 1*A*), clearly distinct from the unbound fraction (~95%) that flowed through the column without trailing, and gave less than 0.5% additional binding when rechromatographed (Fig. 1*B*, *dot-*

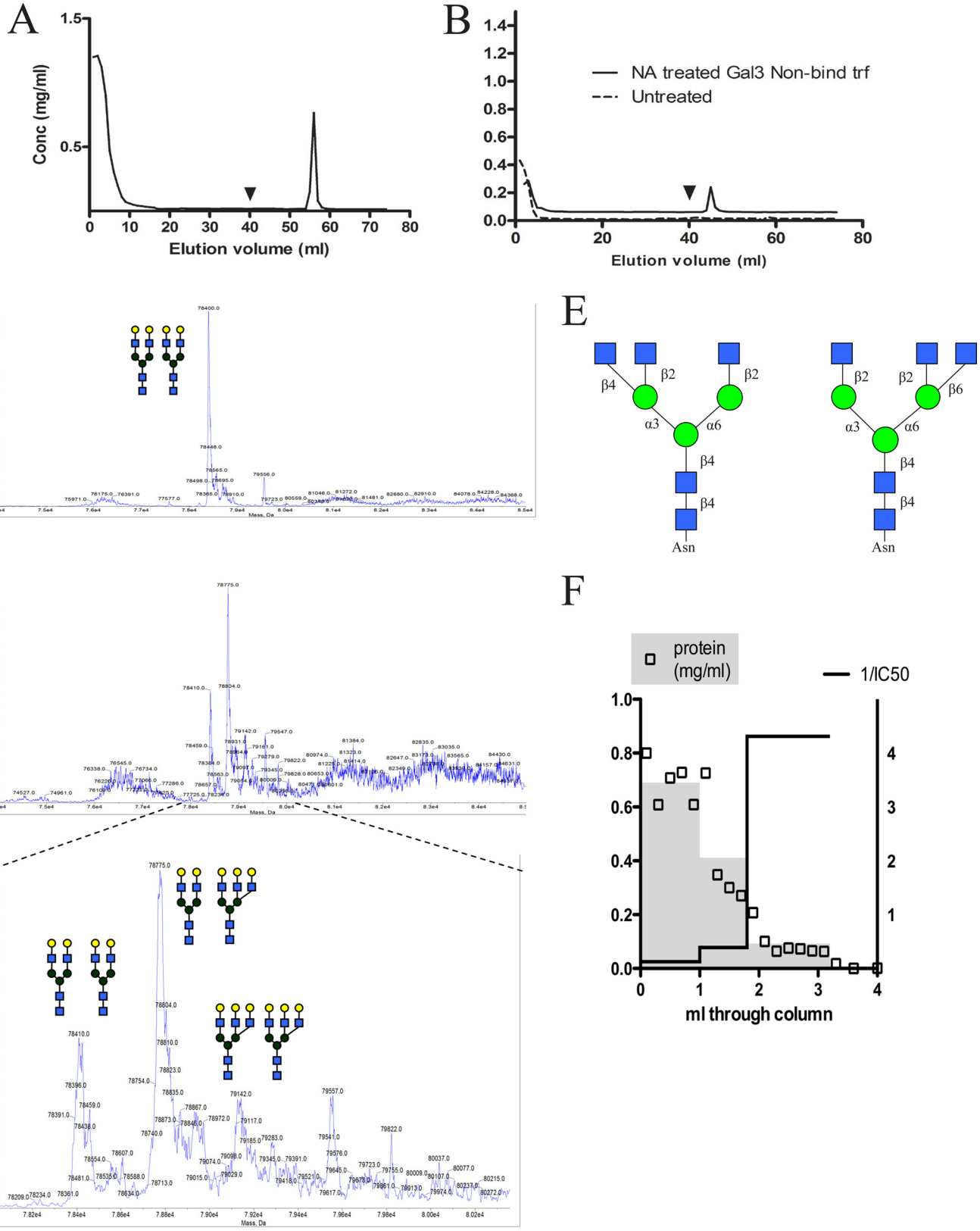

ted line). The potency of galectin-3-bound transferrin as an inhibitor in a fluorescence anisotropy assay corresponded to an average K_d of ~0.5 μM, whereas the unbound fraction had no measurable affinity at all. The galectin-3-bound transferrin carried a clearly different set of *N*-glycans compared with the unbound transferrin, as analyzed by LC-MS of intact transferrin (Fig. 1, *C* and *D*), and previously of glycopeptides (9). The main *N*-glycan of total normal transferrin and galectin-3-unbound transferrin, is by far, a biantennary *N*-glycan, accounting for about 90%, and most of it is not expected to bind galectin-3 as it is capped by 2–6 sialic acids. The main galectin-3-bound transferrin molecules instead carried at least one triantennary *N*-glycan (Fig. 1*D*). This may bind galectin-3 because the third antenna is often capped by 2–3 sialic acids that is tolerated by galectin-3. The mere removal of 2,6-sialic acids from the main bi-antennary *N*-glycan was not sufficient to induce galectin-3 binding, as only another ~4% of the unbound fraction bound after neuraminidase treatment (Fig. 1*B*, *solid line*). Thus, the presence of at least one tri-antennary *N*-glycan is a feature of the main galectin-3 binding glycoforms of transferrin. At least two types of triantennary glycans exist in human transferrin depending on the actions of either *N*-acetylglucoseaminyltransferase (GlcNAcT) IV or V (23). GlcNAcT-IV adds a β4 GlcNAc to the α3 mannose (*left* in Fig. 1*E*), whereas GlcNAcT-V adds a β6 GlcNAc to the α6 mannose (*right* in Fig. 1*E*). The expression of the latter is significantly increased during oncogenic transformation (24) and has been suggested to increase binding to galectin-3 (13, 25). To determine which type of triantennary glycan was responsible for galectin-3 binding of transferrin we used PHA-L affinity chromatography, because glycopeptides carrying the α6 branch but not the α3 branch have been shown to be retarded on a PHA-L column (26). A small fraction of transferrin was retarded on a PHA-L column, and most of the galectin-3 binding potency co-eluted with this fraction (Fig. 1*F*), suggesting that galectin-3 binding of transferrin to a significant extent is mediated by tri-antennary *N*-glycan with the α6 branch. Iron loading of the unfractionated, galectin-3-unbound and galectin-3-bound transferrin was similar, measured as 60, 60, and 50%, respectively. Thus, iron loading does not appear to affect galectin-3 binding of transferrin.

Galectin-3 Binds Increased Levels of Transferrin in Sera from Metastatic Breast Cancer Patients—13 sera from women with metastatic breast cancer (median age 69 years) and 12 sera from healthy women (median age 65 years) were analyzed by affinity chromatography on immobilized galectin-3 (subjects and respective amount of galectin-3 ligands in sera are listed in Table 1). The yield of galectin-3-binding proteins from cancer sera was significantly elevated ($p < 0.0001$) compared with healthy sera (average 7.4 *versus* 4.7 mg/ml of serum) (Fig. 2*A*). Galectin-3 has previously been shown to bind a wide range of serum glycoproteins (9, 11) one being transferrin. The concentrations of total and galectin-3-bound transferrin were determined by ELISA. The level of galectin-3-bound transferrin in the cancer sera was on average about twice as high compared with the average for control sera (0.11 *versus* 0.05 mg/ml of sera, Fig. 2*B*). The serum transferrin did not differ significantly due to disease (Fig. 2*C*). Hence, the increase was primarily due to altered glycosylation, because there was a significant increase in percentage of galectin-3-bound transferrin in the cancer sera compared with healthy sera (4.1 *versus* 2.3%, Fig. 2*C*). Moreover, the yields from the cancer patients were compared with various aspects of the available clinical data for each patient (Table 1) including pharmacological treatments (not shown), without finding any significant correlation. There was, however, a trend ($p = 0.0575$) toward a correlation of increase in primary tumor size with more galectin-3-bound transferrin in serum (average: 0.09 mg/ml for <25 mm *versus* 0.13 mg/ml for >25 mm primary tumors).

Galectin-3-bound and -unbound Glycoforms of Transferrin Are Targeted to Kinetically Diverse Endocytic Pathways in Galectin-3 Expressing HFL-1 Cells but Not in Galectin-3-deficient SKBR3 Cells—Galectin-3-binding and non-binding transferrin were labeled with fluorescein or rhodamine, respectively, and added together to cells (Fig. 3, *A* and *B*). In HFL-1 fibroblasts, which express galectin-3, the two followed clearly different intracellular pathways after uptake, with low initial colocalization (~20% by Manders, Fig. 3*A*, *enclosed graph*, and no colocalization after 45–60 min). In SKBR3 breast carcinoma cells, which do not express endogenous galectin-3 (Fig. 3*B* and Ref. 22), the two transferrin forms overlapped (60–80% by Manders) at all time points up to 60 min (Fig. 3*B*).

In HFL-1 cells, significant amounts of galectin-3-binding transferrin were recycled back to the cell surface after 15–20 min, whereas the non-binding transferrin was still present in intracellular vesicles (Fig. 3*A*). After 45 min, none of the galectin-3-binding transferrin could be detected inside the cells, whereas some of the non-binding glycoforms could be observed along the plasma membrane and after 60 min all transferrin appeared to have left the cell (not shown). In SKBR3 cells, colocalization of binding and non-binding transferrin was primarily found in intracellular structures (10 min), showing rapid inter-

FIGURE 1. **Characterization of galectin-3-binding transferrin glycoforms.** *A,* 5 mg of pooled human transferrin was fractionated on a 5-ml column with immobilized galectin-3. Approximately 5% galectin-3-binding transferrin was eluted with lactose (150 mM) after washing with 32 ml of PBS (*arrowhead*). *B,* the galectin-3 non-binding transferrin was treated (—) with *V. cholerae* neuraminidase (0.1 μmol for 1 h at 37 °C (*NA*)) or not treated (- - -), and again analyzed on a galectin-3-coupled affinity column. Removal of sialylations generated an additional 4% of galectin-3-binding transferrin. Galectin-3 non-binding (*C*) and binding transferrin (*D*) from the affinity chromatography as in *A* was desialylated and further analyzed by LC-MS to determine glycan structures. The mass range around 80 kDa is shown, with close of the area of interest for galectin-3-bound transferrin in the *bottom panel*. Each major peak corresponds to an intact transferrin molecule with two *N*-glycans, as shown by schematic structures. Thus, the major species of galectin-3-unbound transferrin has two biantennary glycans, whereas the major peak for galectin-3-bound transferrin has one biantennary and one triantennary. The monosaccharide symbols are as recommended by Consortium for Functional Glycomics: *purple diamond*, *N*-acetylneuraminic acid; *blue square*, *N*-acetylglucosamine; *green ball*, mannose; *yellow ball*, galactose. *E,* schematic figure of two types of triantennary *N*-glycans. *N*-Acetylglucoseaminyltransferase (*GlcNAcT*) IV or V GlcNAcT-IV adds a β4 GlcNAc to the α3 mannose (*left*), whereas GlcNAcT-V adds a β6 GlcNAc to the α6 mannose (*right*). *F,* 1 mg of human transferrin in a volume of 500 μl was added to 400 μl of a column with immobilized *PHA-L*, and 200-μl fractions were collected under continuous elution with PBS (*open squares*). The fractions were pooled into three groups based on retention time and analyzed for protein content (*gray shade*, left *y* axis) and potency to inhibit galectin-3 in a fluorescent anisotropy assay (*line*, *right y* axis). The main inhibitory potency coincides with the third group, a minor pool of retarded fractions.

TABLE 1

Subjects and respective amount of galectin-3 ligands in sera

14 patients with metastatic breast cancer (1–19) and 13 healthy controls (26–49) were analyzed.

	Pathology diagnosis at primary surgery									
Subject	Galectin-3 ligands	Serum transferrin	Galectin-3-bound transferrin	Age	Breast cancer histological type	Grade	Tumor size[a]	Lymph nodes[b]	ER[c]	PgR[d]
	mg/ml serum	*mg/ml*	*mg/ml sera*							
1	6.7	1.4	0.168	74	Ductal	III	2	12/17	Positive	Negative
2	7.1	2.4	0.126	66	Tubuloductal	III	2	0/12	Negative	Negative
3	11.1	3.5	0.096	62	Lobular	II	1	0/13	Positive	Negative
6	5.8	3.6	0.092	42	Ductal	III	2	3/18	Negative	Negative
8	7.4	3	0.116	79	Tubuloductal	II	2	0/9	Negative	Negative
9	6.7	3.5	0.120	64	Lobular	II	1	1/9	Positive	Negative
10	7.3	3.2	0.086	72	Tubuloductal	I	2	ND[e]	Positive	Positive
12	10.5	2.7	0.066	76	Ductal	ND	1	ND	Positive	Negative
13	7.2	4.8	0.100	70	Tubuloductal	II	1	3/11	Positive	Negative
14	6	1.7	0.059	69	Ductal	ND	1	0/11	Positive	Positive
16	8.3	3.8	0.150	65	Ductal	II	2	2/16	Positive	Positive
17	5.6	3.2	0.107	44	Ductal + lobular	III	2	12	Negative	Positive
19	7.1	5.3	0.202	78	Ductal	ND	2	ND	Positive	Positive
26	4.8	3.2	0.022	77						
29	5.1	2.7	0.040	72						
33	3.6	4.4	0.033	55						
34	6.5	1.7	0.032	60						
36	5,8	1.7	0.061	67						
38	4,1	0.9	0.068	64						
40	3.2	3.1	0.010	61						
42	3.4	2.2	0.056	60						
43	7.1	1.9	0.073	70						
44	5.6	3	0.039	60						
47	3.1	4	0.080	65						
49	3.6	3.2	0.071	66						

[a] Size classes are 1 = <25 mm, 2 = >25 mm.
[b] Nodes with metastasis/nodes examined.
[c] ER, estrogen receptor determined by immunohistochemistry, >10% stained nuclei considered positive.
[d] PgR, progesterone receptor determined by immunohistochemistry, >0% stained nuclei considered positive.
[e] ND, not determined.

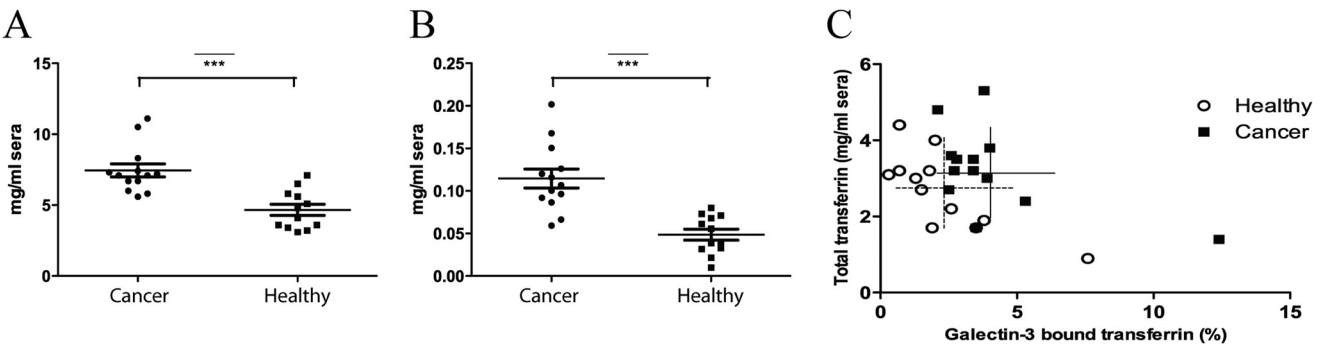

FIGURE 2. **Quantitation of total proteins and galectin-3-bound transferrin in cancer and healthy sera.** *A,* yield of galectin-3-binding proteins (sum of protein amount in bound fractions multiplied by 10 to give mg/ml of the original serum) for sera from 13 cancer patients and 12 healthy individuals. The average for each group is marked by *horizontal lines*, and the difference was statistically significant ($p < 0.0001$). *B,* the concentrations of transferrin in the galectin-3-bound fractions from cancer and healthy sera as determined by ELISA. The average for each group is marked by *horizontal lines*, and the difference was statistically significant ($p < 0.0001$). *C,* initial serum levels of transferrin (*y* axis) compared with % of galectin-3 bound transferrin (*x* axis). The averages and ranges of each parameter are shown by *crossed lines*, *unbroken* for cancer sera and *dashed* for healthy sera. The difference between the % galectin-3-bound transferrin was significant ($p < 0.0001$), whereas the difference between total transferrin was not statistically significant.

nalization (Fig. 3*B*). After 20 min all transferrin had left the membrane and was now concentrated close to the nucleus, still with no difference between the two transferrin subpopulations. After 30 min, transferrin accumulated in close proximity to the cell membrane, suggesting an onset of recycling, supposedly followed by protein secretion because no intracellular staining could be found after 60 min (not shown). Moreover, galectin-3-binding transferrin showed almost total colocalization (90%) with endogenous galectin-3 during endocytosis in HFL-1 cells, whereas non-binding transferrin only colocalized with galectin-3 to a minor degree (20%) (Fig. 3*C*). To examine whether galectin-3 acts as a receptor by binding to transferrin glycoforms at the cell surface, binding of galectin-3-binding transferrin to MCF-7 cells known to express high levels of both the transferrin receptor (CD71) and the surface galectin-3 (27, 28) were analyzed using flow cytometry (Fig. 3*D*). The amount of galectin-3-binding transferrin at the cell surface was significantly reduced by addition of non-binding glycoforms (~50%), whereas a high concentration of (150 mM) lactose, known to completely disrupt galectin-transferrin binding (Fig. 1*A*), was less potent (~20% reduction) (Fig. 3*D*, *top panel*), suggesting that both glycoforms compete for the same receptor. Furthermore, both galectin-3-bound and -unbound transferrin showed distinct overlap (90%) with the CD71 at all time points (not shown). The degree of labeling was similar between the binding and non-binding glycoforms (3.08 *versus* 3.16 mol of fluoresce-

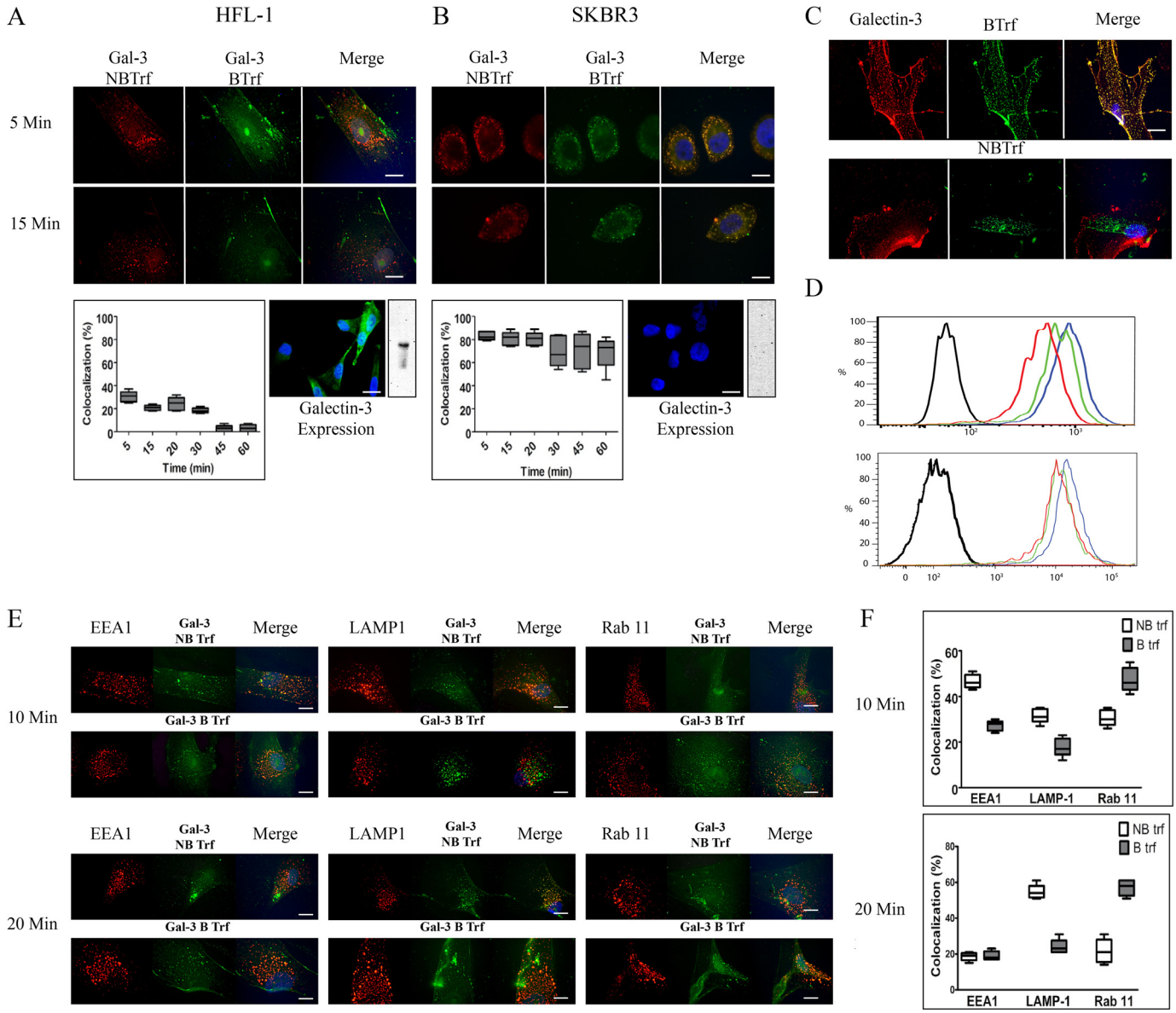

FIGURE 3. **Endocytosis and intracellular trafficking of galectin-3 non-binding (*NB*) and -binding (*B*) transferrin.** HFL-1 (*A*) or SKBR3 (*B*) cells were incubated with 1 μM rhodamine-labeled galectin-3 non-binding transferrin (Gal-3-NB Trf, *red*) or fluorescein-labeled galectin-3-binding transferrin (Gal-3 BTrf) *green*) for 5 min at 37 °C to allow internalization, and then medium was changed to prevent continuous uptake. Endocytosis was stopped at 5, 15, 20, 30, 45, or 60 min by addition of ice-cold PBS (only 5 and 15 min shown). Cells were fixed in paraformaldehyde, nuclei were stained *blue* with Hoechst, and cells were observed by deconvolution fluorescence microscopy (×100 magnification). Colocalization of galectin-3-binding and non-binding transferrin is revealed by the overlap of signals in merged images (*yellow*). Calculated percentage overlap (average of 5 images of each individual experiment) according to Manders after background correction is shown in the *enclosed boxes* for each cell line below the microscopy panels. To the *right* of these, galectin-3 expression examined with immunocytochemistry of permeabilized cells and Western blot of total cell lysates using anti-galectin-3 antibody is shown. *C*, HFL-1 cells were incubated for 10 min with either galectin-3-binding (*top*) or non-binding (*bottom*) fluorescein-labeled transferrin (*green*), and stained with anti-galectin-3 antibody (*red*), and analyzed with deconvolution fluorescence microscopy. *Scale bar* represents 10 μm. *D,* histograms showing MFI of MCF-7 cells incubated with 1 μM rhodamine-labeled galectin-3-binding transferrin (*top panel*) and activated protein C-conjugated anti-galectin-3 (*lower panel*) and analyzed with flow cytometry. Cells were either untreated (*blue line*) in the presence of 150 mM lactose (*green line*) or 5 μM unlabeled galectin-3 non-binding transferrin (*red line*). Unstained cells are shown in *black*. Cells were kept on ice throughout the experiment to prevent uptake. *E,* HFL-1 cells were incubated with 1 μM fluorescein-labeled galectin-3-binding or non-binding transferrin (*green*) for 5 min at 37 °C to allow internalization to occur. Endocytosis was stopped after 10 (*top*) or 20 (*bottom*) min and cells were permeabilized and stained with anti-EEA-1, anti-LAMP-1, or anti-Rab11 (*red*, Alexa 594) and analyzed with deconvolution fluorescence microscopy. *F,* percent overlap according to Manders based on experiments shown in *E* (average of 5 images of each individual experiment). *Scale bar* represents 10 μm. Nuclei were visualized with DAPI (*blue*) for all panels in *A–C* and *E*).

in/mol of transferrin and 2.84 and 2.62 mol of rhodamine/mol of transferrin). Moreover, comparable results were observed when exchanging fluorophores between the transferrin glycoforms (galectin-3-binding and non-binding transferrin labeled with rhodamine or fluorescein, respectively) ruling out confounding effects of the fluorophore.

For preliminary identification of the intracellular pathways taken by the two subpopulations of transferrin (galectin-3 bound and non-bound) (*green* in Fig. 3*E*) we used markers for different endosomal compartments (*red* in Fig. 3*E*) and quantitated the overlap according to Manders (Fig. 3*F*). After 10 min, both showed overlap with EEA1, a marker of early endosomes

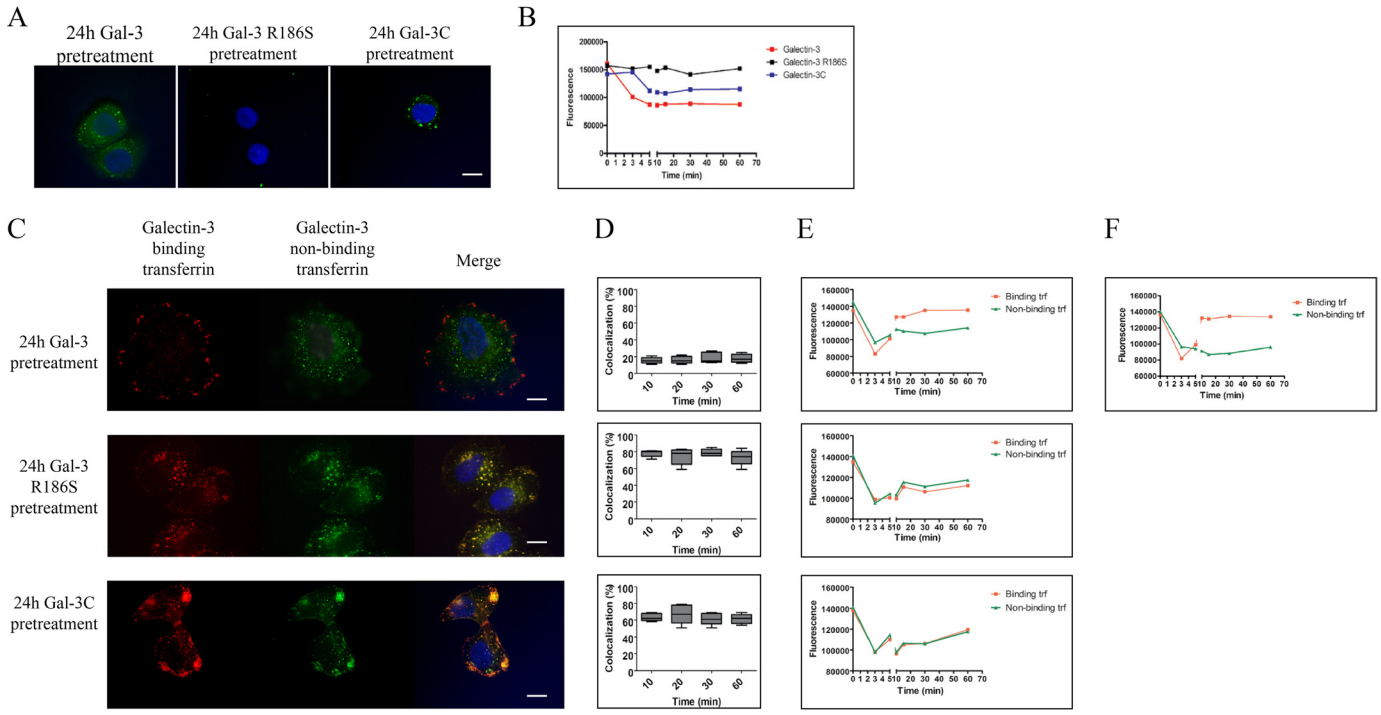

FIGURE 4. **Endocytosis of transferrin in galectin-3-deficient SKBR3 cells pretreated with exogenously added galectin-3 for 24 h.** *A,* SKBR3 cells were incubated with 1 μM fluorescein-labeled galectin-3, galectin-3 mutant R186S (deficient in affinity for LacNAc), and the C-terminal of galectin-3 (*galectin-3C*). Endocytosis was stopped after 24 h, and cells were analyzed with deconvolution fluorescence microscopy. *B,* fluorescence intensities in SKBR3 growth medium, where a decrease indicates uptake of galectins by the cells, with the first (0–5 min) and last parts (15–65 min) on different time scales. *C,* SKBR3 cells were either untreated (Fig. 3*B*) or pretreated with galectin-3, galectin-3 R186S, or galectin-3C for 24 h followed by incubation with 1 μM rhodamine-labeled galectin-3-binding (*red*) and fluorescein-labeled non-binding (*green*) transferrin for 5 min at 37 °C to allow internalization to occur. Endocytosis was stopped after 20 min and analyzed with deconvolution fluorescence microscopy. *Yellow* staining in the merged images confirms eventual overlap. *Scale bar* represents 10 μm. Nuclei were visualized with DAPI (*blue*) for all panels in *A* and *C*. *D,* percent overlap at different time points according to Manders (average of 5 images of each individual experiment of *C*). *E,* the different galectin pretreated SKBR3 cells (as described for *panel C*) were incubated with 1 μM rhodamine-labeled galectin-3 non-binding transferrin (*red*) or fluorescein-labeled galectin-3-binding transferrin (*green*) for 5 min at 37 °C to allow internalization, and then medium was changed to prevent continuous uptake. Fluorescence intensities in removed medium were analyzed using POLARstar Fluorescence polarization microplate reader. Fluorescence intensities of rhodamine-labeled galectin-3-binding (*red*) or fluorescein-labeled non-binding transferrin (*green*) remaining in the medium after different times, as a measure of uptake by the cells (decrease) and subsequent release after recycling (increase), with the first (0–5 min) and last parts (15–65 min) on different time scales. *F,* fluorescence intensities in growth medium from galectin-3-pretreated SKBR3 cells as for *panel E*, but supplemented with U18666A.

where transferrin is known to go initially (6); this was more prominent for the galectin-3 non-binding (~45%) compared with the binding (~30%) fraction. After 20 min, overlap with EEA1 had decreased and the non-binding transferrin overlapped with LAMP-1 (~50%) and the galectin-3-binding transferrin with Rab11 (~60%). Rab11 is a marker and regulator of recycling endosomes (29), a compartment in the main sorting route of transferrin (6), and is also known to overlap with intracellular galectin-3 in Madin-Darby canine kidney cells (30) and SKBR3 cells (22). LAMP-1 is a marker of late endosomes, which can, albeit not typically, be visited by transferrin (4). However, we found partial colocalization (~30%) between LAMP-1 and EEA1, suggesting that some of the transferrin overlap with LAMP-1 could reflect a distinct population of double labeled endosomes. In further support of these different sorting routes for the different transferrin glycoforms, treatment of HFL-1 cells with the Niemann-Pick disease mimicking drug U18666A, retained galectin-3 non-binding transferrin inside the cell, whereas galectin-3-binding transferrin continued to be recycled (not shown). Together, these observations support a model with two types of recycling routes, a faster for galectin-3-bound transferrin with a return rate to the plasma membrane of 10–20 min and a slower, U18666A inhabitable route, with a return rate of about 30 min (31).

Galectin-3 Preloaded SKBR3 Cells Acquire the Ability of Galectin-3-regulated Transferrin Trafficking—To examine the role of cellular galectin-3 in transferrin sorting, we preloaded galectin-3-deficient SKBR3 cells with exogenously added galectin-3, by a procedure shown to restore galectin-dependent functions in other galectin-deficient cells (32). Galectin-3 was rapidly taken up by the SKBR3 cells, as expected from other cell types (33, 34) (Fig. 4*B*), and was after 24 h found in both large and small vesicular structures in the cytosol (Fig. 4*A*). Galectin-3 R186S mutant, deficient in binding to LacNAc and glycoproteins, was not taken up at all (Fig. 4*A*, *middle panel*). Galectin-3C, a truncated form of galectin-3 lacking the N-terminal domain and cross-linking ability, was taken up but less efficient than wild type galectin-3, and assembled only in larger structures after 24 h (Fig. 4*A*, *right panel*).

SKBR3 cells treated with galectin-3 for 24 h gained the ability to sort galectin-3-bound and -unbound transferrin differently (Fig. 4*C*, *top panel*), as they showed very little overlap (Fig. 4*D*, *top panel*), and galectin-3-bound transferrin was recycled more rapidly and efficiently (Fig. 4*E*, *top panel*). By contrast, in galec-

tin-3 R186S pretreated cells both transferrin glycoforms were endocytosed with no divergence in their sorting (~80% overlap) and recycling rate (Fig. 4, *C–E*, *middle panels*). Also in galectin-3C-pretreated cells the two transferrin glycoforms mainly overlapped (Fig. 4, *C–E*, *bottom panels*), but the intracellular pattern differed (Fig. 4*C*, *bottom panel*) with accumulations of overlapping transferrin aggregates near the cell membrane as the main feature, along with smaller accumulation of non-overlapping glycoforms in the cytosol. Treatment of galectin-3-loaded SKBR3 cells with U18666A specifically blocked recycling of the non-binding glycoform (Fig. 4*F*), as described above for HFL-1 cells, suggesting comparable sorting machinery in these cells. Together these data show that the different intracellular targeting of the two transferrin glycoforms can be rescued by preloading the galectin-3-deficient cells with galectin-3, and that both the carbohydrate-binding activity and the N-terminal domain of galectin-3 are required for this, conceivably for cross-linking with *e.g.* vesicular membranes as previously proposed (35, 36).

DISCUSSION

The binding of transferrin to its receptor at the cell surface does not require its *N*-glycans (7), but the role of *N*-glycans in the subsequent intracellular sorting of transferrin has not been studied before. The present results clearly demonstrate that two sets of glycoforms of transferrin can be sorted into different pathways after uptake into cells by endocytosis, and that this different sorting is dependent on galectin-3. The recycling rate (10–20 min) and the colocalization with Rab11 of galectin-3-bound transferrin most resembles the transferrin taking the route via perinuclear recycling endosomes in previous studies (2–4, 6, 31), whereas the path for the galectin-3-unbound transferrin appears slower. None of them behave as for direct fast recycling (2–4 min) from early endosomes (2–5). However, the cell type and resolution of the present studies may have made this hard to see, and the pathways and rates found in one particular cell type will also depend on how much and what species of galectin-3 it expresses and perhaps other factors. For example, alterations in the sphingolipid composition of trafficking vesicles have been shown to alter transferrin sorting by redirecting it to LAMP-positive endosomes (37). In addition, it should also be noted that LAMP-1 transiently visits early endosomes after synthesis, and this may explain the unexpected distinct overlap of the unbound transferrin with LAMP-1-positive endosomes (38). Furthermore, many defining model studies have been done using human transferrin in animal model cells transfected with human transferrin receptor (2–4, 6, 31), such as CHO cells that express moderate levels of hamster galectin-3 and Madin-Darby canine kidney cells that express very high levels of dog galectin-3, but it is not known how well these galectin-3 species interact with human transferrin.

Importantly, galectin-3 endocytosis appears to be cell specific (39), consequently transferrin targeting might vary between cell type and tissue environment. Galectin-3 has recently been shown to be rapidly internalized by vascular endothelial cells (40) and macrophages (39) appearing in EEA1 positive endosomes within 10–15 min and then partitioned into two routes, either recycling (through Rab11 positive endosomes) or targeting to the LE/lysosomes (LAMP-1 positive endosomes). However, the dynamics of these endocytic pathways partly differed depending on cell type. Moreover, the partial targeting of galectin-3 to the LE/lysosomes may explain the minor overlap of galectin-3-bound transferrin with LAMP-1 found here. Furthermore, it has been shown that iron load can influence the kinetics of transferrin endocytosis (41). However, variance in iron loading cannot account for the different sorting of galectin-3-bound and -unbound transferrin observed here, because it was similar in the two fractions (50 and 60%, respectively). Still, because the transferrin is pooled from human blood, the small difference in iron loading may reflect a different metabolic history of the two transferrin fractions, *i.e.* galectin-3-binding transferrin has delivered more of its iron.

It seems most likely that both the galectin-3-binding and non-binding glycoforms of transferrin bind initially and about equally well to the transferrin receptor. The affinity of the galectin interactions is most likely too low to compete with the high affinity transferrin-CD71 interaction (42). In support of this there is a significant overlap between galectin-3-binding transferrin and the transferrin receptor, and galectin-3-non-binding transferrin competes for it (Fig. 4*D*). In all, it is likely that galectin-3 binding of transferrin becomes decisive after transferrin binding of its receptor and subsequent endocytosis into early endosomes. Binding of galectin-3 to the transferrin receptor itself (43),[4] might also contribute. Here galectin-3 binding of transferrin appears to divert the complex directly to Rab11-positive endosomes for faster recycling kinetics. Intriguingly, Rab11 endosomes have previously been recognized as candidate compartments for galectins and glycosylated cargo proteins (44). In support of this we observe a significant overlap between galectin-3-binding transferrin and Rab11 not seen for the non-binding glycoforms.

The fact that there was an enrichment of triantennary complex *N*-glycans in the galectin-3-bound fraction and that neuraminidase treatment did not cause a significant increase in binding suggest that the third antenna is required for galectin-3 binding of transferrin. The increased galectin-3 binding of the PHA-L-retarded fractions imply that the mannose α6 branch at least to some extent is involved in this interaction. This could also explain the increased yield of galectin-3-binding glycoforms of transferrin but also total serum proteins found in sera from metastatic breast cancer patients. Amplified branching due to increased expression of GlcNAcT-V responsible for adding the β6 GlcNAc to the α6 mannose is considered a hallmark of cancer progression (45), and has been shown to facilitate tumor growth in various *in vivo* and *in vitro* models (46–48). Moreover, Lau *et al.* (48) showed that the expression of GlcNAcT-V served as a regulator of the strength of the association of the EGF receptor and galectin-3 lattice and subsequently a modulator of the choice between growth and arrest. It is speculated that the preferential elongation of the β6 GlcNAc with poly-*N*-acetyllactosamine is accountable for the increased affinity, this is, however, unlikely to be essential for galectin binding of transferrin here, because of the absence of poly-*N*-

[4] Y. Qian, J. Stegmayr, and H. Leffler, unpublished data.

acetyllactosamine in serum glycoproteins (11). Instead, galectin-3 binding of transferrin appears to be mediated through binding to the β6 GlcNAc extended with a β1–4-galactose, either exposed or terminated with a α2,3-NeuAc.

Because of their wide range of important biological activities, galectins are enigmatic in terms of identifying a central physiological function, if only one exists. The importance of galectin-glycan interactions in various cellular events, especially intracellular and intercellular trafficking of proteins, has been shown by numerous studies (13, 15, 16, 30, 48). Hence, the role in intracellular guidance of glycoproteins shown here and by others emerges as a feasible explanation for these multifaceted activities. We have previously shown that the interaction of haptoglobin with galectin-1 is decisive for its intracellular trafficking (11). Moreover, this process is disturbed in cancer, because glycosylation changes associated with oncogenic transformation cause a significant increase in galectin-1-binding haptoglobin glycoforms. It should be remarked that the increase of galectin-3-binding glycoproteins and glycoforms of transferrin observed here is only based on a limited number of patients, and the clinical value of this may be of less importance. The purpose here was only to assess if there was any difference between sera from patients with severe cancer and healthy controls, and to set that finding into a biological context. Hence, even if a seemingly trivial fraction of transferrin as seen here is sorted into a different intracellular pathway after uptake this small percentage appears to go up in metastatic breast cancer. Such regulation could be critical for tumor cells, in which effective iron metabolism is crucial, because rapidly dividing cancer cells have a higher requirement for iron than their normal counterparts (49, 50). Furthermore, altered cell metabolism could also influence the glycosylation machinery (15, 48). The hexosamine pathway regulates the activities of the Golgi branching enzymes by production of their donor substrate UDP-GlcNAc and this metabolic control has been shown to fine-tune galectin-3 regulation of glycoprotein receptors (48). Hence it is possible that the altered cell metabolism associated with cancer accounts for the increase in galectin-3-binding glycoforms of transferrin and may serve as a regulator of transferrin trafficking. Also, other pathological conditions known to be associated with transferrin glycosylation changes, such as alcohol-induced liver injury (8) and hepatoma (51), may cause altered binding to galectin-3. Hence, under pathological circumstances, understanding the mechanisms that determine the time transferrin spends inside a cell would be of particular interest to identify design criteria for improving the drug delivery efficacy of transferrin, *e.g.* in anti-cancer therapy (6). Moreover, some earlier studies using transferrin as a endocytic marker will now also have to be reinterpreted in light of the fact that transferrin cannot be regarded as homogenous, and instead contains at least two different fractions with different recycling rates and paths. As a final point, the different trafficking of galectin-3-bound and -unbound transferrin points to the possibility of a previously unrecognized level of physiological regulation. Even though altered glycosylation is a feature of most cancers the functional implications of these are still enigmatic. Here we provide the first evidence that such alterations can influence the intracellular trafficking of transferrin through its binding of the endogenous lectin galectin-3.

Acknowledgments—We thank Barbro Kahl-Knutson for excellent technical support. We also thank Mårten Fernö and Håkan Olsson, Department of Oncology, Lund University, for providing serum samples from breast cancer patients and matched controls.

REFERENCES

1. Richardson, D. R., and Ponka, P. (1997) The molecular mechanisms of the metabolism and transport of iron in normal and neoplastic cells. *Biochim. Biophys. Acta* **1331,** 1–40
2. Sheff, D., Pelletier, L., O'Connell, C. B., Warren, G., and Mellman, I. (2002) Transferrin receptor recycling in the absence of perinuclear recycling endosomes. *J. Cell Biol.* **156,** 797–804
3. Sheff, D. R., Daro, E. A., Hull, M., and Mellman, I. (1999) The receptor recycling pathway contains two distinct populations of early endosomes with different sorting functions. *J. Cell Biol.* **145,** 123–139
4. Maxfield, F. R., and McGraw, T. E. (2004) Endocytic recycling. *Nat. Rev. Mol. Cell Biol.* **5,** 121–132
5. Grant, B. D., and Donaldson, J. G. (2009) Pathways and mechanisms of endocytic recycling. *Nat. Rev. Mol. Cell Biol.* **10,** 597–608
6. Mayle, K. M., Le, A. M., and Kamei, D. T. (2012) The intracellular trafficking pathway of transferrin. *Biochim. Biophys. Acta* **1820,** 264–281
7. Mason, A. B., Miller, M. K., Funk, W. D., Banfield, D. K., Savage, K. J., Oliver, R. W., Green, B. N., MacGillivray, R. T., and Woodworth, R. C. (1993) Expression of glycosylated and nonglycosylated human transferrin in mammalian cells. Characterization of the recombinant proteins with comparison to three commercially available transferrins. *Biochemistry* **32,** 5472–5479
8. Flahaut, C., Michalski, J. C., Danel, T., Humbert, M. H., and Klein, A. (2003) The effects of ethanol on the glycosylation of human transferrin. *Glycobiology* **13,** 191–198
9. Cederfur, C., Salomonsson, E., Nilsson, J., Halim, A., Oberg, C. T., Larson, G., Nilsson, U. J., and Leffler, H. (2008) Different affinity of galectins for human serum glycoproteins. Galectin-3 binds many protease inhibitors and acute phase proteins. *Glycobiology* **18,** 384–394
10. Dennis, J. W., Granovsky, M., and Warren, C. E. (1999) Glycoprotein glycosylation and cancer progression. *Biochim. Biophys. Acta* **1473,** 21–34
11. Carlsson, M. C., Cederfur, C., Schaar, V., Balog, C. I., Lepur, A., Touret, F., Salomonsson, E., Deelder, A. M., Fernö, M., Olsson, H., Wuhrer, M., and Leffler, H. (2011) Galectin-1-binding glycoforms of haptoglobin with altered intracellular trafficking, and increase in metastatic breast cancer patients. *PloS one* **6,** e26560
12. Carlsson, M. C., Balog, C. I., Kilsgård, O., Hellmark, T., Bakoush, O., Segelmark, M., Fernö, M., Olsson, H., Malmström, J., Wuhrer, M., and Leffler, H. (2012) Different fractions of human serum glycoproteins bind galectin-1 or galectin-8, and their ratio may provide a refined biomarker for pathophysiological conditions in cancer and inflammatory disease. *Biochim. Biophys. Acta* **1820,** 1366–1372
13. Partridge, E. A., Le Roy, C., Di Guglielmo, G. M., Pawling, J., Cheung, P., Granovsky, M., Nabi, I. R., Wrana, J. L., and Dennis, J. W. (2004) Regulation of cytokine receptors by Golgi N-glycan processing and endocytosis. *Science* **306,** 120–124
14. Leffler, H., Carlsson, S., Hedlund, M., Qian, Y., and Poirier, F. (2004) Introduction to galectins. *Glycoconj. J.* **19,** 433–440
15. Ohtsubo, K., Takamatsu, S., Minowa, M. T., Yoshida, A., Takeuchi, M., and Marth, J. D. (2005) Dietary and genetic control of pancreatic beta cell glucose transporter-2 glycosylation promotes insulin secretion in suppressing the pathogenesis of type 2 diabetes. *Glycobiology* **15,** 1196–1196
16. Delacour, D., Greb, C., Koch, A., Salomonsson, E., Leffler, H., Le Bivic, A., and Jacob, R. (2007) Apical sorting by galectin-3-dependent glycoprotein clustering. *Traffic* **8,** 379–388
17. Sörme, P., Kahl-Knutsson, B., Huflejt, M., Nilsson, U. J., and Leffler, H. (2004) Fluorescence polarization as an analytical tool to evaluate galectin-ligand interactions. *Anal. Biochem.* **334,** 36–47

18. Cumpstey, I., Salomonsson, E., Sundin, A., Leffler, H., and Nilsson, U. J. (2007) Studies of arginine-arene interactions through synthesis and evaluation of a series of galectin-binding aromatic lactose esters. *Chembiochem* **8,** 1389–1398
19. Carlsson, A., Wingren, C., Ingvarsson, J., Ellmark, P., Baldertorp, B., Fernö, M., Olsson, H., and Borrebaeck, C. A. (2008) Serum proteome profiling of metastatic breast cancer using recombinant antibody microarrays. *Eur. J. Cancer* **44,** 472–480
20. O'Brien, J. F., Lacey, J. M., and Bergen, H. R., 3rd (2001) Detection of hypo-*N*-glycosylation using mass spectrometry of transferrin. in *Current Protocols in Human Genetics*, Vol. 54, pp. 17.4.1–17.4.9, John Wiley & Sons, Inc., New York.
21. Crack, J. C., Green, J., Le Brun, N. E., and Thomson, A. J. (2006) Detection of sulfide release from the oxygen-sensing [4Fe-4S] cluster of FNR. *J. Biol. Chem.* **281,** 18909–18913
22. Salomonsson, E., Carlsson, M. C., Osla, V., Hendus-Altenburger, R., Kahl-Knutson, B., Oberg, C. T., Sundin, A., Nilsson, R., Nordberg-Karlsson, E., Nilsson, U. J., Karlsson, A., Rini, J. M., and Leffler, H. (2010) Mutational tuning of galectin-3 specificity and biological function. *J. Biol. Chem.* **285,** 35079–35091
23. Hatton, M. W., März, L., Berry, L. R., Debanne, M. T., and Regoeczi, E. (1979) Bi- and tri-antennary human transferrin glycopeptides and their affinities for the hepatic lectin specific for asialo-glycoproteins. *Biochem. J.* **181,** 633–638
24. Buckhaults, P., Chen, L., Fregien, N., and Pierce, M. (1997) Transcriptional regulation of *N*-acetylglucosaminyltransferase V by the *src* oncogene. *J. Biol. Chem.* **272,** 19575–19581
25. Demetriou, M., Granovsky, M., Quaggin, S., and Dennis, J. W. (2001) Negative regulation of T-cell activation and autoimmunity by Mgat5 *N*-glycosylation. *Nature* **409,** 733–739
26. Cummings, R. D., and Kornfeld, S. (1982) Characterization of the structural determinants required for the high affinity interaction of asparagine-linked oligosaccharides with immobilized *Phaseolus vulgaris* leukoagglutinating and erythroagglutinating lectins. *J. Biol. Chem.* **257,** 11230–11234
27. Satelli, A., Rao, P. S., Gupta, P. K., Lockman, P. R., Srivenugopal, K. S., and Rao, U. S. (2008) Varied expression and localization of multiple galectins in different cancer cell lines. *Oncol. Rep.* **19,** 587–594
28. Jiang, X. P., Elliott, R. L., and Head, J. F. (2010) Manipulation of iron transporter genes results in the suppression of human and mouse mammary adenocarcinomas. *Anticancer Res.* **30,** 759–765
29. Ullrich, O., Reinsch, S., Urbé, S., Zerial, M., and Parton, R. G. (1996) Rab11 regulates recycling through the pericentriolar recycling endosome. *J. Cell Biol.* **135,** 913–924
30. Delacour, D., Cramm-Behrens, C. I., Drobecq, H., Le Bivic, A., Naim, H. Y., and Jacob, R. (2006) Requirement for galectin-3 in apical protein sorting. *Curr. Biol.* **16,** 408–414
31. Pipalia, N. H., Hao, M., Mukherjee, S., and Maxfield, F. R. (2007) Sterol, protein and lipid trafficking in Chinese hamster ovary cells with Niemann-Pick type C1 defect. *Traffic* **8,** 130–141
32. Stechly, L., Morelle, W., Dessein, A. F., André, S., Grard, G., Trinel, D., Dejonghe, M. J., Leteurtre, E., Drobecq, H., Trugnan, G., Gabius, H. J., and Huet, G. (2009) Galectin-4-regulated delivery of glycoproteins to the brush border membrane of enterocyte-like cells. *Traffic* **10,** 438–450
33. Furtak, V., Hatcher, F., and Ochieng, J. (2001) Galectin-3 mediates the endocytosis of β-1 integrins by breast carcinoma cells. *Biochem. Biophys. Res. Commun.* **289,** 845–850
34. Carlsson, S., Carlsson, M. C., and Leffler, H. (2007) Intracellular sorting of galectin-8 based on carbohydrate fine specificity. *Glycobiology* **17,** 906–912
35. Herrmann, J., Turck, C. W., Atchison, R. E., Huflejt, M. E., Poulter, L., Gitt, M. A., Burlingame, A. L., Barondes, S. H., and Leffler, H. (1993) Primary structure of the soluble lactose binding lectin L-29 from rat and dog and interaction of its non-collagenous proline-, glycine-, tyrosine-rich sequence with bacterial and tissue collagenase. *J. Biol. Chem.* **268,** 26704–26711
36. Nieminen, J., Kuno, A., Hirabayashi, J., and Sato, S. (2007) Visualization of galectin-3 oligomerization on the surface of neutrophils and endothelial cells using fluorescence resonance energy transfer. *J. Biol. Chem.* **282,** 1374–1383
37. Shakor, A. B., Taniguchi, M., Kitatani, K., Hashimoto, M., Asano, S., Hayashi, A., Nomura, K., Bielawski, J., Bielawska, A., Watanabe, K., Kobayashi, T., Igarashi, Y., Umehara, H., Takeya, H., and Okazaki, T. (2011) Sphingomyelin synthase 1-generated sphingomyelin plays an important role in transferrin trafficking and cell proliferation. *J. Biol. Chem.* **286,** 36053–36062
38. Rohrer, J., Schweizer, A., Russell, D., and Kornfeld, S. (1996) The targeting of Lamp1 to lysosomes is dependent on the spacing of its cytoplasmic tail tyrosine sorting motif relative to the membrane. *J. Cell Biol.* **132,** 565–576
39. Lepur, A., Carlsson, M. C., Novak, R., Dumić, J., Nilsson, U. J., and Leffler, H. (2012) Galectin-3 endocytosis by carbohydrate independent and dependent pathways in different macrophage like cell types. *Biochim. Biophys. Acta* **1820,** 804–818
40. Gao, X., Liu, D., Fan, Y., Li, X., Xue, H., Ma, Y., Zhou, Y., and Tai, G. (2012) The two endocytic pathways mediated by the carbohydrate recognition domain and regulated by the collagen-like domain of galectin-3 in vascular endothelial cells. *PloS One* **7,** e52430
41. Zhang, H.-L., Li, Y.-Q., Zhang, M.-Z., and Zhao, Y.-D. (2010) Real-time observation of the effect of iron on receptor-mediated endocytosis of transferrin conjugated with quantum dots. *J. Biomed. Opt.* **15,** 045003–045003
42. Ward, J. H., Kushner, J. P., and Kaplan, J. (1982) Transferrin receptors of human fibroblasts. Analysis of receptor properties and regulation. *Biochem. J.* **208,** 19–26
43. Stillman, B. N., Hsu, D. K., Pang, M., Brewer, C. F., Johnson, P., Liu, F.-T., and Baum, L. G. (2006) Galectin-3 and galectin-1 bind distinct cell surface glycoprotein receptors to induce T cell death. *J. Immunol.* **176,** 778–789
44. Straube, T., von Mach, T., Honig, E., Greb, C., Schneider, D., and Jacob, R. (2013) pH-dependent recycling of galectin-3 at the apical membrane of epithelial cells. *Traffic* **14,** 1014–1027
45. Lau, K. S., and Dennis, J. W. (2008) *N*-Glycans in cancer progression. *Glycobiology* **18,** 750–760
46. Demetriou, M., Nabi, I. R., Coppolino, M., Dedhar, S., and Dennis, J. W. (1995) Reduced contact-inhibition and substratum adhesion in epithelial cells expressing GlcNAc-transferase V. *J. Cell Biol.* **130,** 383–392
47. Granovsky, M., Fata, J., Pawling, J., Muller, W. J., Khokha, R., and Dennis, J. W. (2000) Suppression of tumor growth and metastasis in Mgat5-deficient mice. *Nat. Med.* **6,** 306–312
48. Lau, K. S., Partridge, E. A., Grigorian, A., Silvescu, C. I., Reinhold, V. N., Demetriou, M., and Dennis, J. W. (2007) Complex *N*-glycan number and degree of branching cooperate to regulate cell proliferation and differentiation. *Cell* **129,** 123–134
49. Richardson, D. R., Kalinowski, D. S., Lau, S., Jansson, P. J., and Lovejoy, D. B. (2009) Cancer cell iron metabolism and the development of potent iron chelators as anti-tumour agents. *Biochim. Biophys. Acta* **1790,** 702–717
50. Kwok, J. C., and Richardson, D. R. (2002) The iron metabolism of neoplastic cells. Alterations that facilitate proliferation? *Crit. Rev. Oncol. Hematol.* **42,** 65–78
51. Yamashita, K., Koide, N., Endo, T., Iwaki, Y., and Kobata, A. (1989) Altered glycosylation of serum transferrin of patients with hepatocellular carcinoma. *J. Biol. Chem.* **264,** 2415–2423